Challenging exclusive top quark pair production at low and high luminosity LHC

Daniel E. Martins,[1,*] Marek Tasevsky,[2,†] and Victor P. Gonçalves[1,‡]

[1]*Instituto de Física e Matemática, Universidade Federal de Pelotas (UFPel), Caixa Postal 354, CEP 96010-090, Pelotas, RS, Brazil*

[2]*Institute of Physics of the Czech Academy of Sciences, Na Slovance 2, 18221 Prague 8, Czech Republic*

(Received 2 February 2022; accepted 20 May 2022; published 2 June 2022)

The elastic production of top quark pairs in pp collisions at low and high luminosity regimes is investigated in detail. We extend the study performed in [V. P. Gonçalves *et al.*, Phys. Rev. D **102**, 074014 (2020).] which has demonstrated that the sum of two semiexclusive $t\bar{t}$ production modes, namely in photon-Pomeron ($\gamma\mathbb{P}$) and Pomeron-Pomeron ($\mathbb{P}\mathbb{P}$) interactions, can be experimentally measured when the $t\bar{t}$ system decays semileptonically, $t\bar{t} \to jjbl\nu_l\bar{b}$, both forward protons are tagged and a low amount of pile-up is present. In this study we focus on separating individual channels and a special attention is paid to the situation at high-luminosity LHC environment. We observe that the separation of the $\mathbb{P}\mathbb{P}$ and $\gamma\gamma$ events is a challenging task, especially at high amounts of pile-up even with an optimistic 10 ps resolution of timing detectors. In contrast, the $\gamma\mathbb{P}$ signal is relatively well separable from all backgrounds at low levels of pile-up, allowing us to discover the elastic $t\bar{t}$ production and probe, for the first time, the production of a top quark pair in the $\gamma\mathbb{P}$ interactions. The diffractive photoproduction of such a complex system as the $t\bar{t}$ pair hence can be used not only to study diffractive properties of the scattering amplitude but also to search for new physics beyond the Standard Model, and consequently to be a solid part of the physics program of forward proton detectors at LHC.

DOI: 10.1103/PhysRevD.105.114002

I. INTRODUCTION

The top quark plays a central role in the Standard Model (SM) and is generally considered to be an excellent probe for new physics beyond Standard Model (BSM). It is the heaviest particle of the SM, with a mass close to the scale of the electroweak symmetry breaking, implying that the top production and decays at colliders are very sensitive to the presence of BSM phenomena (see, e.g., Refs. [1,2]). Such aspects have strongly motivated studies of top quark production at the LHC, where top quarks are produced with a high production rate in inelastic proton-proton collisions, where both incident protons break up and a large number of particles is produced in addition to the top quarks (for recent experimental results see, e.g., Refs. [3–8]). It turned out that the analysis of top quark production in inelastic collisions generally involve serious backgrounds, thus making the search for new physics a hard task. An alternative, recently proposed in Ref. [9] (see also Ref. [10]), is the study of top quark production in pp collisions characterized by intact protons in the final state. In what follows, this process will be denoted as *elastic* top quark production and a schematic diagram is represented in Fig. 1. The basic idea is that the incident protons emit color singlet objects $\mathcal{S}_1$ and $\mathcal{S}_2$, which can be a quasireal photon γ or a Pomeron $\mathbb{P}$, the protons remain intact and scatter with some energy loss ξ in a very small angle from the beam pipe. This way the top quark pair can thus be produced in $\gamma\gamma$, $\gamma\mathbb{P}$ or $\mathbb{P}\mathbb{P}$ interactions. While the $\gamma\gamma$ interaction is a purely exclusive process, where only the $t\bar{t}$ pair is present in the final state, in $\gamma\mathbb{P}$ and $\mathbb{P}\mathbb{P}$ interactions the pair is accompanied by Pomeron remnants (denoted by Y in Fig. 1) when it is modeled as a quasireal color singlet particle with partonic structure and such processes are denoted as semiexclusive. Elastic production is also characterized by the presence of two rapidity gaps, i.e., two regions devoid of hadronic activity separating the intact very forward protons from the central system. In principle, events associated to the elastic top quark production can be clearly distinguished from the inelastic events by detecting the scattered protons in spectrometers placed in the very forward region close to the beam pipe, such as the ATLAS Forward Proton detector (AFP) [11,12] and the

*dan.ernani@gmail.com
†Marek.Tasevsky@cern.ch
‡barros@ufpel.edu.br

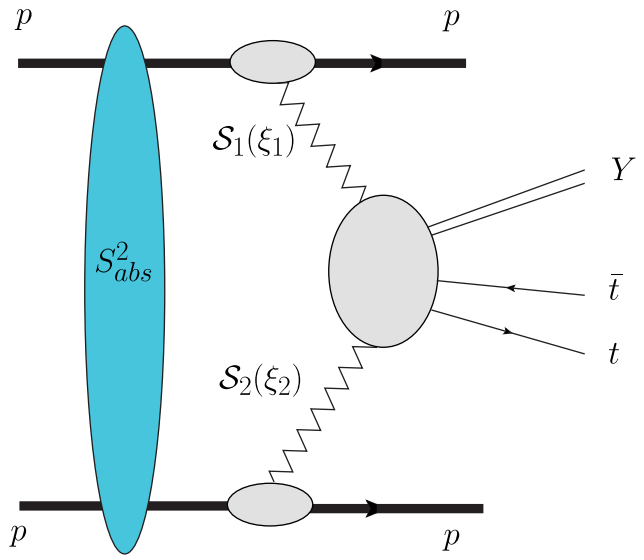

FIG. 1. Elastic top pair production in pp collisions, where $\mathcal{S}_1$ and $\mathcal{S}_2$ denote a color singlet object [photon (γ) or Pomeron ($\mathbb{P}$)], ξ_i is the fractional momentum loss of incident protons and Y are the Pomeron remnants present in $\gamma\mathbb{P}$ and $\mathbb{P}\mathbb{P}$ interactions.

CMS–Totem Precision Proton Spectrometer (CT–PPS) [13], and selecting events with two rapidity gaps in the central detector. However, in reality, the separation of elastic events is a challenge due to the presence of extra pp interactions per bunch crossing, usually called pile-up, in high luminosity pp collisions at the LHC. The pile-up generates additional tracks that in general destroy the signature associated to two rapidity gaps and increase the background stemming from the inelastic top quark pair produced in a different primary vertex.

In our previous article [9], we have performed the first comprehensive study of the elastic top quark pair production in pp collisions at $\sqrt{s} = 13$ TeV taking into account the current detector acceptances and resolutions as well as the pile-up effects expected for the next run of the LHC. Good prospects for observing the elastic signal over a mixture of inclusive and combinatorial background were achieved for all luminosity scenarios considered, although a good separation between the two is observed for rather low amounts of pile-up, typically lower than 50. In particular in Ref. [9] we showed that the separation is feasible for a sum of two semiexclusive production modes, $\gamma\mathbb{P}$ and $\mathbb{P}\mathbb{P}$, when the $t\bar{t}$ system decays semi-leptonically, $t\bar{t} \to jjbl\nu_l\bar{b}$, both forward protons are tagged and a low amount of pile-up is present. Our goal in this paper is to improve and extend the analysis performed in Ref. [9] by considering additional exclusivity cuts and utilizing the time-of-flight (TOF) detectors for suppressing the combinatorial background coming from pile-up. We will focus on separating the $t\bar{t}$ final state produced in semiexclusive ($\gamma\mathbb{P}$ and $\mathbb{P}\mathbb{P}$) or even exclusive ($\gamma\gamma$) processes from backgrounds at the low—and high—luminosity LHC environments. As we will demonstrate below, the separation of the $\mathbb{P}\mathbb{P}$ and $\gamma\gamma$ events will be a challenging task, especially at high amounts of pile-up even with an optimistic 10 ps resolution of timing detectors. In contrast, the events associated to the top quark production in $\gamma\mathbb{P}$ interactions can be relatively well separable from all backgrounds at low levels of pile-up. Such results indicate that the elastic $t\bar{t}$ production can be discovered in a near future at the LHC and that an experimental analysis of this process will be able to probe, for the first time, the diffractive photoproduction of top quark pairs. Moreover, such a perspective opens the possibility to search for new physics beyond the Standard Model in this process.

This paper is organized as follows. In next section, we present a brief review of the formalism for the elastic top pair production pp collisions. In Sec. III we discuss details of the selection of events and cuts implemented in our analysis, concentrating on collisions at $\sqrt{s} = 13$ TeV in the low—and high—luminosity regimes. In Sec. IV we present our results for the distributions of the fractions of proton momentum loss and invariant mass and our predictions for the effective cross sections. Moreover, the significance for the distinct processes is estimated considering different amounts of pile-up. Finally, in Sec. V we summarize our main findings.

II. FORMALISM

For completeness, in this section we will present a brief review of the formalism needed to describe the elastic top pair production in $\gamma\gamma$, $\gamma\mathbb{P}$, and $\mathbb{P}\mathbb{P}$ interactions and refer the reader to Ref. [9] for a more detailed discussion. A well-known aspect is that an ultrarelativistic proton acts as a source of almost real photons and that the associated photon spectrum can be computed using the equivalent photon approximation [14]. In a similar way, one can associate a Pomeron flux to the incident protons, with the Pomeron being usually modeled as a quasireal color singlet particle with a partonic structure [15]. As a consequence, the total cross section for the elastic top pair production can be factorized in terms of the equivalent flux of photons and Pomerons into the proton projectiles and the photon-photon, photon–Pomeron or Pomeron–Pomeron production cross section. Denoting by $\mathcal{S}_{1,2}$ the generic color singlet object, the cross section can be represented in a schematic way as in Fig. 1 and expressed as follows

$$\sigma(pp \to p \otimes t\bar{t}Y \otimes p) \propto S^2_{abs} \times f_{\mathcal{S}_1}(\xi_1) \times f_{\mathcal{S}_2}(\xi_2) \times \hat{\sigma}(\mathcal{S}_1\mathcal{S}_2 \to t\bar{t}), \quad (1)$$

where $\otimes$ represents the presence of a rapidity gap in the final state, ξ_i is the fraction of the incident proton energy carried by the color singlet object $\mathcal{S}_i$ and $f_{\mathcal{S}_i}$ is the equivalent photon or Pomeron distribution of the proton. Moreover, Y denote the Pomeron remnants present in $\gamma\mathbb{P}$

and $\mathbb{PP}$ interactions and S^2_{abs} is the rapidity gap survival factor, which takes into account additional soft interactions between the incident protons which leads to an extra production of particles that destroy the rapidity gaps in the final state [16].

In order to estimate the total cross sections and associated distributions for the elastic top pair production, one has to assume a model for the equivalent photon and Pomeron distributions as well as for the survival factor. Following Ref. [9], we will use the photon flux from Ref. [14], where an analytical expression is derived. Moreover, the Pomeron distribution is expressed in terms of the diffractive parton distributions, whose evolution is described by the DGLAP evolution equations and are determined from events with a rapidity gap or intact proton, mainly at HERA collider [17]. As in Ref. [9] we will express these quantities assuming the validity of the resolved Pomeron model [15] and will describe the diffractive parton distributions by the parametrization obtained by the H1 Collaboration at HERA, denoted as the fit A in Ref. [18]. As emphasized in Ref. [9], the treatment of S^2_{abs} for $\gamma\gamma$, $\gamma\mathbb{P}$ and $\mathbb{PP}$ interactions is still a theme of intense debate due to the nonperturbative nature of the additional interactions (see, e.g., Ref. [19]). We will assume that the hard process associated to the top pair production occurs on a short enough timescale such that physics that generate the additional particles can be factorized, which allows us to parametrize the absorption effects in terms of a global constant factor. While for the photon-photon and photon-Pomeron collisions the contribution of the additional soft interactions is expected to be small due to the long range of the electromagnetic interaction, it is non-negligible for Pomeron-Pomeron collisions and imply the violation of the QCD hard scattering factorization theorem for diffraction in pp collisions [20]. In our analysis, following Ref. [9], we will assume $S^2_{abs} = 1$ for $\gamma\gamma$ and $\gamma\mathbb{P}$ interactions. Recent studies [21–23] have derived a smaller value for the survival factor in $\gamma\gamma$ interactions. As a consequence, our predictions can be considered to be an upper bound for the elastic top pair production in photon-photon interactions. In contrast, for $\gamma\mathbb{P}$ interactions, such assumption is a very good approximation, since the resolved Pomeron model is able to describe the diffractive charm photoproduction measured at HERA. On the other hand, the modeling and magnitude of S^2_{abs} for $\mathbb{PP}$ interactions are still open questions, with its value being typically of the order of 1%–5% for LHC energies. As in previous studies for single and double diffractive production [24–28] we will assume $S^2_{abs} = 0.03$ for Pomeron-Pomeron interactions as predicted in Ref. [29] but we will also try to address the question of what is the impact on our results if a larger value is considered.

A comment about the top production close to the threshold is in order. In the last decades, several groups have demonstrated that the calculation of the $t\bar{t}$ cross sections close to threshold in e^-e^+ and pp collisions using fixed-order perturbation theory in the strong coupling α_s needs to be complemented by a resummation of the Coulomb effects (see, e.g., Refs. [30–36]). Such effects, associated to the strong attraction between the quark and antiquark, imply an enhancement of the cross section close to the threshold, with the magnitude of the threshold cross section and the position of its peak being sensitive to the top quark mass and width, as well as to the value of α_s. In particular, the normalization of the cross section is expected to be increased by 20%–30% in a small range of invariant masses close to the threshold. Such predictions are expected to be probed in the future e^-e^+ colliders, where the main observable is the total cross section as a function of the center-of-mass energy, which can be adjusted to probe the threshold region. In contrast, in hadronic colliders, one considers the invariant mass distribution of the $t\bar{t}$ pairs, where, however, it becomes harder to probe the impact of the Coulomb effects. Unfortunately, as we will see later, it is also challenging for (semi)-exclusive top production in $\gamma\gamma$, $\gamma\mathbb{P}$ and $\mathbb{PP}$ interactions considered in this paper, since the achieved event yields do not allow us to make a fine enough binning needed to study details of the $m_{t\bar{t}}$ spectrum around the threshold.

III. EXPERIMENTAL PROCEDURE

The procedure used to separate the elastic signal from backgrounds, represented mainly by pile-up, is based on that described in detail in Ref. [9], so here we only remind the main steps and then we will describe two new cuts introduced in this analysis. In Ref. [9] we have demonstrated that background processes $\gamma\gamma \to WW$ and $\gamma\mathbb{P} \to Wt$ can safely be neglected in the case of our signal induced by $\gamma\mathbb{P}$ and $\mathbb{PP}$ interactions. That allows us to consider as backgrounds for each signal process the inclusive production of $t\bar{t}$ pair and the other two elastic processes, all overlaid with pile-up (as an example, in the case of $\gamma\mathbb{P} \to t\bar{t}$ signal, the backgrounds are inclusive $t\bar{t}$, $\gamma\gamma \to t\bar{t}$ and $\mathbb{PP} \to t\bar{t}$, all evaluated including pile-up effects). To estimate the statistical significance, σ, and signal to background ratio, S/B, we consider three luminosity scenarios in terms of $\langle\mu\rangle$ and $\mathcal{L}$ where $\langle\mu\rangle$ represents the average number of pile-up interactions per event (or the instantaneous luminosity) and $\mathcal{L}$ is the integrated luminosity. We assume $\mathcal{L}$ to be 10, 300, and 4000 fb^{-1} for $\langle\mu\rangle = 5$, 50, and 200, respectively, the last one corresponding to the assumed conditions at HL-LHC. It is appropriate to note that compared to the approach adopted in Ref. [9], namely to use a simple formula $S/\sqrt{B}$ to estimate significances, in this study we use the formula based on Asimov data set [37] which reflects the reality more reliably and which reduces to the simple ratio above if $S \ll B$.

The separation of the elastic $t\bar{t}$ signal from backgrounds at proton-proton collisions at center-of-mass system energy

of $\sqrt{s} = 13$ TeV proceeds in three steps: first we select the central system as in the inclusive processes, then we apply exclusivity criteria and finally we add two new cuts, with the aim to separate individual processes from each other. In the first step, we concentrate on the so-called semileptonic $t\bar{t}$ decay, $t\bar{t} \to jjbl\nu_l\bar{b}$, in the second step, we require both forward protons to be detected by forward proton detectors (FPDs), to be processed by time-of-flight (ToF) detectors with an assumed resolution of 10 ps and the decay products of the $t\bar{t}$ pair to be accompanied by a low number of particles. The third step consists of cuts on the proton transverse momentum and a 2-dimensional cut in the $(m_X, m_{t\bar{t}})$ plane where m_X is the missing mass evaluated from forward proton measurements and $m_{t\bar{t}}$ is the mass of the $t\bar{t}$ system measured by the central detector.

All three signal processes are generated using the forward physics Monte Carlo (FPMC) [38], while the inclusive $t\bar{t}$ background is generated by MadGraph5 [39]. Each event is then properly mixed with such a number of pile-up interactions that corresponds to the studied luminosity scenario (e.g., for the $(\langle\mu\rangle, \mathcal{L}) = (5, 10)$ point, the actual number of overlaid pile-up events is coming from a Poisson distribution with the mean of 5.0). A sample for the pile-up mixing consists of 200 thousands of minimum bias events generated by PYTHIA8 [40] including multiparton interactions. Detector effects are incorporated and this pile-up mixing is done using DELPHES3.5 [41] with input cards with CMS detector specifications. Where available, ATLAS cards are used for systematic studies. For $\langle\mu\rangle = 5$ and 50, DELPHES package provides cards with both, the ATLAS and CMS parameters, while for $\langle\mu\rangle = 200$, we used a CMS card tuned in recent HL-LHC studies [42]. For all, the elastic and inclusive $t\bar{t}$ processes, the mass of the top quark is set to the value of 174.0 GeV. For FPDs we assume a fully efficient reconstruction in the range $0.015 < \xi_{1,2} < 0.15$, where $\xi_{1,2} = 1 - p_{z1,2}/E_{\text{beam}}$ is the fractional proton momentum loss on either side of the interaction point (side 1 or 2) and p_{z1} is the longitudinal momentum of the scattered proton on the side 1. This, in principle, allows one to measure masses of the central system by the missing mass method, $m_X = \sqrt{\xi_1\xi_2 s}$, starting from about 200 GeV. Large event samples of the aforementioned processes have been generated, each of at least 200,000 events, corresponding—in the case of signal processes—to integrated luminosities that sufficiently exceed the assumed ones in the three considered luminosity scenarios.

All cuts used in the first two steps are elaborated in Ref. [9]. One can find there details about jet definition, b-tagging, about lepton definition and isolation, about number of tracks originating in a narrow region around the primary vertex and far from all objects in the final state (so called z-vertex veto). Here we would like to only remind how we make use of the ToF detector. First we evaluate a probability to see an intact proton from one minimum bias event in the FPD ξ-acceptance on one side and after, eventually, applying the proton p_T cut, P_{ST}. Based on this probability, we then calculate combinatorial factors representing rates of fake double-tagged events for the three studied working points of $\langle\mu\rangle$ and for various options for proton p_T cut. Finally the ToF suppression factors are enumerated for each combination of $\langle\mu\rangle$ and proton p_T cut, under the assumption that the time resolution of ToF is $\sigma_{\text{ToF}} = 10$ ps and the signal is collected in a $\Delta t = \pm 2\sigma_{\text{ToF}}$ window. More details about the ToF method and the $\langle\mu\rangle$-dependence of this combinatorial background can be found in Refs. [43–45]. Given the large Δt collection window, the efficiency of the signal collection at $\langle\mu\rangle = 0$ is close to 100%. In this study we assume a very good granularity of the ToF detector and no $\langle\mu\rangle$ dependence of the signal or background collection efficiency.

In the third step, we apply two additional cuts with the aim to separate individual processes from each other. The cut on proton p_T is potentially a powerful cut if pile-up is not present since it helps to separate the elastic processes among each other on one hand and all elastic processes from the background formed by the inclusive production plus pile-up on the other hand. The reason for the former is a different p_T spectrum of proton which emits photon from that which emits Pomeron, see Fig. 2. The reason for the latter is a decrease of the rate of fake double-tagged events as a natural consequence of a decrease of the probability P_{ST} whenever additional cuts on the forward proton are imposed. Another potential background rejector is based on the fact that the individual processes studied here occupy different regions in a 2-dimensional (m_X, $m_{t\bar{t}}$) plane where m_X is the missing mass evaluated from forward proton measurements and $m_{t\bar{t}}$ is the mass of the $t\bar{t}$ system measured in the central detector. The situation at $\langle\mu\rangle = 5$ is illustrated in Fig. 3 which suggests a relatively good potential for separation of the $\gamma\gamma$ signal from all other processes in general. When plotting these distributions, the effective cross sections of the mix of inclusive and pile-up events are already scaled by the corresponding rates of fake double tagged events and by ToF suppression factors.

All the cuts considered in our analysis are summarized in Table I. Basically, we require the following:

(i) In total at least four not-overlapping jets with $E_{T,\text{jet}} > 25$ GeV and $|\eta_{\text{jet}}| < 2.5$ (for HL-LHC, we consider the extended coverage $|\eta| < 4.0$ of the upgraded tracker).

(ii) At least one electron or muon (τ decays included) with $E_{\text{T,l}} > 25$ GeV and $|\eta_{\text{l}}| < 2.5(4.0)$ isolated from all four jets, $\Delta R_{\text{l,j}} > 0.2$.

(iii) At least two b-tagged jets. A jet is b-tagged if a B-hadron (generator level) or a b-quark (detector level) is found inside the jet.

(iv) Exactly two forward protons, each in the FPD acceptance $0.015 < \xi_{1,2} < 0.15$.

(v) Number of tracks with $p_{T,\text{trk}} > 0.2$ GeV and $|\eta_{\text{trk}}| < 2.5(4.0)$ in the distance $|z_{\text{trk}} - z_{\text{vtx}}| < 1$ mm from

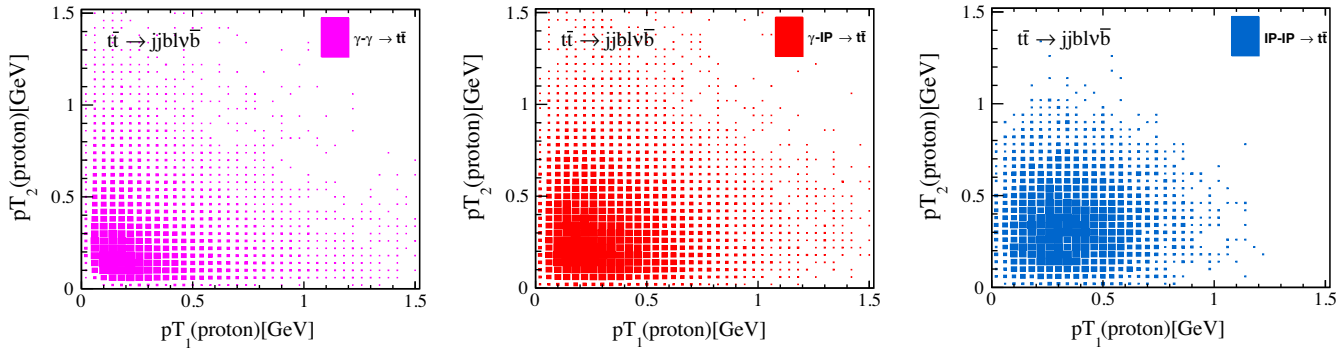

FIG. 2. 2-dimensional distribution of the transverse momentum of proton on one side from the interaction point versus that on the opposite side, after applying cuts in Table I up to the row corresponding to the ξ acceptance inclusively and without considering pile-up effects. Predictions for the signal processes ($\gamma\gamma$ on the left, $\gamma\mathbb{P}$ in the middle and $\mathbb{P}\mathbb{P}$ on the right) are obtained with FPMC and are scaled by effective cross sections corresponding to the set of applied cuts.

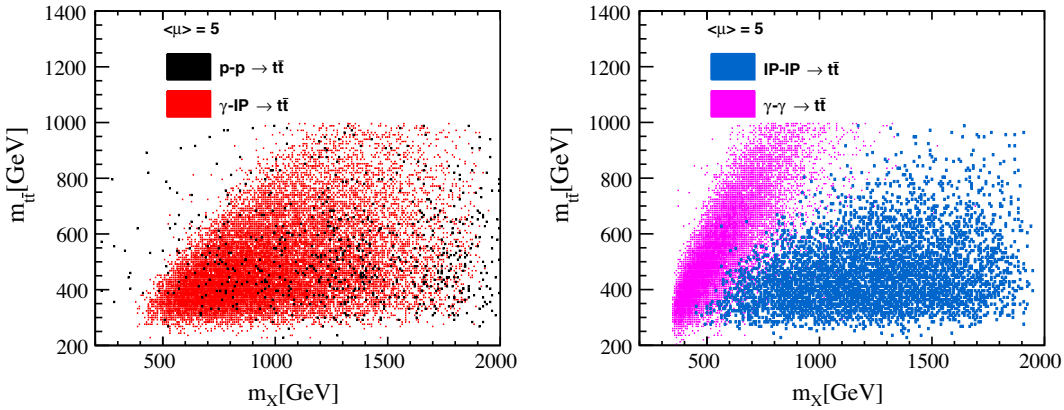

FIG. 3. 2-dimensional distribution of the central $t\bar{t}$ system mass measured by forward proton detectors (m_X) versus that measured by central detector ($m_{t\bar{t}}$) after applying all cuts in Table I up to the row corresponding to the ξ acceptance inclusively. Predictions, scaled by effective cross sections corresponding to the set of applied cuts, are obtained with FPMC for processes $\gamma\gamma$, $\gamma\mathbb{P}$ and $\mathbb{P}\mathbb{P}$, while MadGraph5 +PYTHIA8 is used for the inclusive $t\bar{t}$ production. All processes are mixed with pile-up with $\langle\mu\rangle = 5$.

the primary vertex and $\Delta R_{\mathrm{trk,j}} > 0.4$ from the four jets and $\Delta R_{\mathrm{trk,l}} > 0.2$ from one lepton must be smaller than a given value X.

(vi) p_T of each proton detected in FPD must be smaller than a given value Y.

TABLE I. Cuts used in this analysis. The extended η coverage is considered only for the HL-LHC scenario.

Cut
$N_{\mathrm{jet}} \geq 4$ ($E_T > 25$ GeV, $\lvert\eta\rvert < 2.5(4.0)$)
$N_{e/\mu} \geq 1$ ($E_T > 25$ GeV, $\lvert\eta\rvert < 2.5(4.0)$)
$\Delta R(\mathrm{e}/\mu, \mathrm{jet}) > 0.2$
$N_{\mathrm{b-jet}} \geq 2$
$0.015 < \xi_{1,2} < 0.15$
$N_{\mathrm{trk}}(p_{\mathrm{T}} > 0.2\ \mathrm{GeV}, \lvert\eta\rvert < 2.5(4.0), \lvert\Delta z\rvert < 1\ \mathrm{mm}) \leq X$
$p_T^{\mathrm{proton}} < Y$
Optimal area in the (m_X, $m_{t\bar{t}}$) plane

(vii) Optimal area in the (m_X, $m_{t\bar{t}}$) plane is found for each signal process. We proceed in a rather simple manner and select—merely on a visual basis—the optimal area as a continuous part of the 2D plane with an advantageous S/B ratio. For each process we tried several areas and kept the one giving the best significance but it is clear that better results can be obtained if more sophisticated methods are used. One can usually try to find Fischer discriminant or to perform regression analysis or, if more variables can be used to separate signal from background, one can make use of machine learning techniques, e.g., boosted decision trees and neural networks.

IV. RESULTS

Areas of population for individual processes shown in Fig. 3 clearly demonstrate that the process $\gamma\gamma$ can in principle be isolated well from all other processes. Nevertheless due to its extremely low effective cross

section, in order to collect a reasonable event yields, we have to only consider large integrated and hence instantaneous luminosities and thus consider only the luminosity scenarios $(\langle\mu\rangle, \mathcal{L}) = (50, 300)$ and (200, 4000). Then the good isolation seen at low values of $\langle\mu\rangle$ is completely washed out due to the inclusive background points scattered all around the area, as expected from flat mass distributions for this type of background when pile-up is not negligible (see Figs. 2 and 3 in Ref. [9] for masses larger than 500 GeV). The other additional cut on proton p_T turns out to be futile in improving statistical significance. The largest observed values are around 0.1 for no cut on proton P_T and $N_{\text{trk}} \leq 15$ for both $\langle\mu\rangle = 50$ and $\langle\mu\rangle = 200$.

As far as the $\gamma\mathbb{P}$ process is concerned, the extraction of an optimal area in the $(m_X, m_{t\bar{t}})$ plane turns out to be useful only marginally when $\langle\mu\rangle = 5$ and it was abandoned completely at higher amounts of pile-up for the same reasons as mentioned above. In general, the forward proton p_T cut does not improve the situation since—unlike for the $\gamma\gamma$ and $\mathbb{P}\mathbb{P}$ processes—the p_T spectrum is broader due to the fact that one proton emits photon and the other Pomeron. At $\langle\mu\rangle = 5$, this signal is well observable over all backgrounds, with a significance of 3.4 for $N_{\text{trk}} \leq 25$. The significances are lower for larger amounts of pile-up. At $\langle\mu\rangle = 50$ a maximum significance of 2.1 is obtained for $N_{\text{trk}} \leq 25$ and at $\langle\mu\rangle = 200$, a maximum significance of 2.3 is achieved for $N_{\text{trk}} \leq 30$ when the extended $|\eta| < 4.0$ coverage for the upgraded tracker is taken into account. For the last case, we studied three scenarios regarding the z-veto region and minimum p_T of tracks counted inside it, namely 1 mm and 0.2 GeV (the nominal configuration used for lower $\langle\mu\rangle$ values), 0.5 mm and 0.5 GeV, and 0.2 mm and 0.5 GeV, and we observed practically no improvement. Very similar numbers are obtained with the ATLAS card where available ($\langle\mu\rangle = 5$ and 50).

Only modest significances are obtained when trying to separate the $\mathbb{P}\mathbb{P}$ process. Although here the proton p_T cut plays a more important role than searching for the optimal area in the $(m_X, m_{t\bar{t}})$ plane, its effect is still rather marginal and the best significance of 0.9 was achieved for no cut on proton p_T and $N_{\text{trk}} \leq 20$. At such low amounts of pile-up it is the $\gamma\mathbb{P}$ process that plays a role of the main background thanks to its relatively large cross section and similar behavior in the $(m_X, m_{t\bar{t}})$ or proton (p_{T1}, p_{T2}) planes—see Figs. 2 and 3. However, the ξ distributions of these two processes differ at low ξ values—see Fig. 4. A slightly improved significance of 1.2 is achieved after cutting out the low-ξ part of the spectrum: $0.05 < \xi_{1,2} < 0.15$. For a nearly same set of cuts (namely no cut on proton p_T, $N_{\text{trk}} \leq 20$ and $0.05 < \xi_{1,2} < 0.15$) the best significance of 1.1 is reached at the pile-up of $\langle\mu\rangle = 50$. For the HL-LHC luminosity scenario, the maximum significance of 1.2 is achieved for the $0.2 < p_T^{\text{proton}} < 0.7$ GeV and $20 < N_{\text{trk}} < 40$ cut configuration, when the enhanced tracker $|\eta| < 4.0$

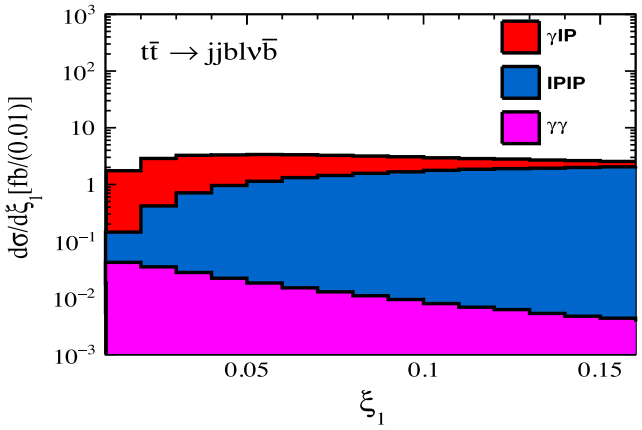

FIG. 4. Distribution of fraction of proton momentum loss on one side (the distribution of the same quantity on the other side is nearly identical), after applying cuts in Table I up to the row corresponding to the number of b-tagged jets inclusively and without considering pile-up effects. Predictions for the signal processes $\gamma\gamma$, $\gamma\mathbb{P}$ and $\mathbb{P}\mathbb{P}$ are obtained with FPMC and are scaled by effective cross sections corresponding to the set of applied cuts.

coverage is considered. The three cut sets in the (z-veto region, track p_T) space give very similar results.

As we pointed out above, production of the $t\bar{t}$ system in collision of two Pomerons suffers from a large uncertainty in the value of S^2. To stay on the safe side, we take conservatively a relatively low value of 3% for our nominal results above. Doubling this value would simply double the signal event yield, while leaving all backgrounds unchanged. This would then lead to significances of 2.4, 2.2 and 1.6 for the three luminosity scenarios, (5, 10), (50, 300), and (200, 4000), respectively.

The effective cross sections after applying individual cuts from Table I and scaling by the rates of fake double tagged events and by the ToF suppression, are summarized in Table II.

A comment about a possible top quark mass measurement using elastic processes is in order. As we stated in Ref. [9], for a sensible measurement of the top quark mass, one would need a sufficient amount of signal events and a very low level of background contamination. In the most promising scenario where the $\gamma\mathbb{P}$ process is separated from all other backgrounds overlaid with pile-up of $\langle\mu\rangle = 5$ with the significance of 3.4, the signal to background ratio in terms of event yields from a data sample corresponding to an integrated luminosity of 10 fb^{-1} is 11.1/7.5. Such statistics are still not sufficient to sensibly complement the top quark mass measurements in inclusive channels.

In what follows, we will study the dependence of our results on the resolution of the ToF detector. This property of the ToF detector is clearly key for all measurements of elastic processes at LHC. We remind that AFP reached a time resolution $\sigma_{\text{ToF}} = 20$–22 ps in Run 2 (with a rather

TABLE II. Cut flow for the effective cross sections in femtobarns for the case where the semiexclusive signal process is $\gamma\mathbb{P}$ and the process $\mathbb{P}\mathbb{P}$ and inclusive $t\bar{t}$ production are backgrounds, for three amounts of pile-up, namely $\langle\mu\rangle = 5$, 50, and 200 (for the last, we use the $|\eta| < 4.0$ coverage of the upgraded tracker). The effect of the ξ cut for the inclusive background with pile-up is evaluated as a combinatorial background coming from the rate of fake double-tagged events. Suppression of pile-up effects from using ToF information is based on $\sigma_{\mathrm{ToF}} = 10$ ps and Refs. [43,44].

Process	$\gamma\mathbb{P}(\langle\mu\rangle = 5/50/200)$	$\mathbb{P}\mathbb{P}(\langle\mu\rangle = 5/50/200)$	Incl. $t\bar{t} + \mathrm{PU}(\langle\mu\rangle = 5/50/200)$
Generated cross section [fb]	52.0	29.4	390000.0
$N_{e/\mu} \geq 1$ ($E_T > 25$ GeV, $\|\eta\| < 2.5(4.0)$)	13.1/13.1/18.3	6.9/6.9/9.6	85138.9/80324.4/129753.0
$N_{\mathrm{jet}} \geq 4$ ($E_T > 25$ GeV, $\|\eta\| < 2.5(4.0)$)	4.2/4.6/6.3	2.0/2.2/4.1	33953.4/35150.7/76126.1
$\Delta R(\mathrm{e}/\mu, \mathrm{jet}) > 0.2$	4.2/4.6/6.3	2.0/2.2/4.1	33953.4/35150.7/76116.3
$m_{t\bar{t}} < 1000$ GeV, $m_X > 400$ GeV	3.9/4.2/6.2	2.0/2.2/4.1	28577.3/29406.0/57242.3
$0.015 < \xi_{1,2} < 0.15$	2.5/2.5/3.7	0.7/0.8/1.6	147.7/10215.6/54202.7
ToF suppression	2.5/2.5/3.7	0.7/0.8/1.6	8.4/1094.9/21509.0

low, sub-10% efficiency [46]), whereas CT-PPS time resolution expectations are rather beyond such values. While the performance of the ToF detector in general and as functions of pile-up, time resolution and spatial granularity are studied in detail in Ref. [45], here we illustrate the effect of worsening σ_{ToF} for one specific process and for one specific (most promising) cut scenario giving the significance of 3.4 quoted above, i.e., for the process $\gamma\mathbb{P}$ in the luminosity scenario $(\langle\mu\rangle, \mathcal{L}) = (5, 10)$ and after applying all cuts in the Table I including the optimal area in the $(m_X, m_{t\bar{t}})$ plane and $N_{\mathrm{trk}} \leq 20$ cut. While we assume that the number of events for (semi)exclusive processes does not change with σ_{ToF} at such a small pile-up, the contamination by inclusive process overlaid with pile-up increases almost linearly. In numbers this amounts to 11.1$\gamma\mathbb{P}$ and 1.7 $\mathbb{P}\mathbb{P}$ events, while the inclusive background increases from 2.9 events for 5 ps to 5.8 events for 10 ps and 58 events for 50 ps. This would correspond to a gradual deterioration of significance from 4.0 for 5 ps to 3.4, 2.8, 2.3 and 1.4 for 10, 20, 30 and 50 ps, respectively. In the effort to visualize this σ_{ToF} dependence, in Fig. 5 we plot missing mass spectra m_X for the three processes and five σ_{ToF} values above, but for a slightly different cut scenario, namely for the whole $(m_X, m_{t\bar{t}})$ area available since this simplifies the projection of the 2D-dependence to the 1D m_X-dependence significantly. It should be noted that this simplification decreases the corresponding significances but not dramatically (e.g., 3.0 for 10 ps rather than 3.4 for 10 ps with the optimal 2D area).

Finally it is worth reminding that prospects for separation of the sum of $\gamma\mathbb{P}$ and $\mathbb{P}\mathbb{P}$ processes from all backgrounds remain good, in particular at low pile-up, as emphasized in Ref. [9]. Assuming $\sigma_{\mathrm{ToF}} = 10$ ps, maximal significances reach values of 4.7, 2.7 and 3.0 for the three luminosity scenarios examined in this study, namely for $(\langle\mu\rangle, \mathcal{L}) = (5, 10)$, $(50, 300)$, and $(200, 4000)$, respectively, where for the last, the enhanced tracker coverage is considered. The first two are less favorable than those reported in our initial study [9] which is due mainly to two reasons. First, as explained above, we use the more appropriate formula for significance which is well approximated by the simple ratio $S/\sqrt{B}$ for $S \ll B$ but it gives lower values for $S \approx B$. The second reason is the use of the most recent version of DELPHES. It improves treatment of low-momentum charged particles which, however, leads to distributions of N_{trk} in signal and inclusive background process when both overlaid with pile-up closer to each other than we observed in the version 2.5 used in Ref. [9]. The significance of 3.0 achieved for the HL-LHC conditions promises to keep the semiexclusive production of the $t\bar{t}$ system in the portfolio of potentially interesting and feasible processes for the future of LHC. If the ToF resolution improved to 5 ps at HL-LHC, the statistical significance would even increase to 3.7. This would correspond to a signal event yield of about 16 thousands and a S/B ratio of the order of one per mille. Extracting such a sample of signal from this relatively big pile-up contamination is certainly worth the effort but it will require to measure the latter with a high accuracy (for example by data-driven methods, see, e.g., [47].)

V. SUMMARY

In recent years, it became clear that the precise study of the top quark production and its decay at colliders can shed light on several aspects of the SM and provide a way to search for BSM physics. In general, these studies have been performed considering the top production in inelastic pp collisions, where the incident protons break up and a large of number of particles is produced in addition to the top. A cleaner final state is present when the top is produced by the interaction between color singlet objects emitted by the incident protons. Such elastic top production can be explored considering the AFP and CT-PPS detectors that are installed symmetrically around the interaction point at a distance of roughly 210 m from the ATLAS and CMS detectors. Such a possibility was investigated, for the first time, in Ref. [9] and good prospects for the measurement of

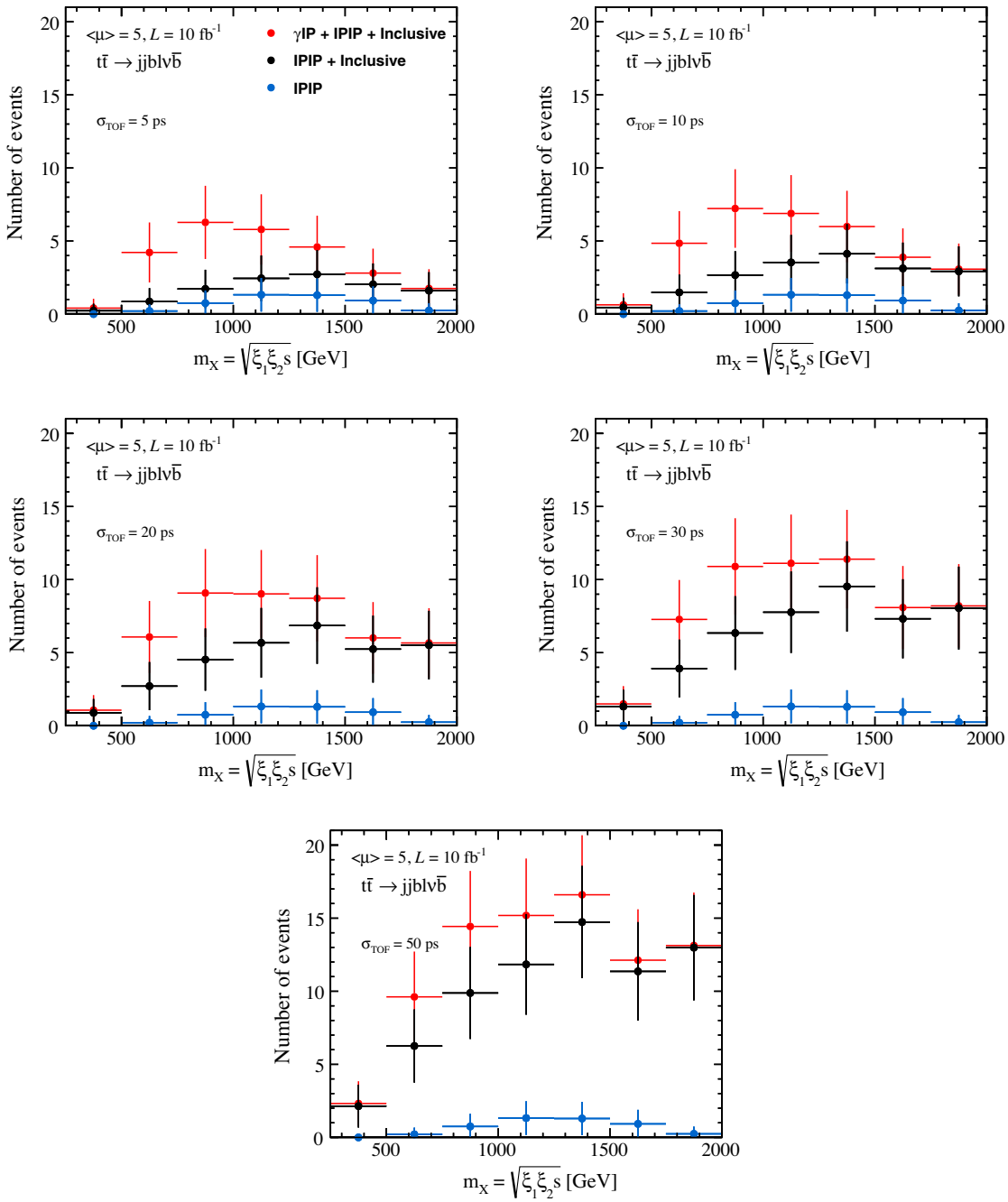

FIG. 5. Separation of $\gamma\mathbb{P}$ as a function of ToF reconstruction, σ_{ToF}. Distribution of missing mass calculated using protons detected in FPDs at generator level after applying cuts in Table I and the $N_{\mathrm{trk}} \leq 20$ cut. For each σ_{ToF} value, a corresponding suppression factor is applied to the inclusive background. Predictions for the two semiexclusive processes $\gamma\mathbb{P}$ and $\mathbb{P}\mathbb{P}$ are obtained with FPMC, while the inclusive $t\bar{t}$ background was generated with MadGraph5+PYTHIA8. All are overlaid with pile-up with $\langle\mu\rangle = 5$ interactions per event and numbers of events correspond to the integrated luminosity of 10 fb^{-1}.

this process were obtained. Such results have motivated the analysis performed here, where we have improved the study considering additional cuts and a more realistic treatment of the detector response.

We studied in detail prospects for measuring the $t\bar{t}$ pair produced in the exclusive ($\gamma\gamma$) and semiexclusive ($\gamma\mathbb{P}$ and $\mathbb{P}\mathbb{P}$) processes. We analyzed three luminosity scenarios, going from a low pile-up running ($\langle\mu\rangle = 5$), through $\langle\mu\rangle = 50$, typical in Run 2 or assumed for the upcoming Run 3, up to assumed conditions at HL-LHC, $\langle\mu\rangle = 200$. With the help of DELPHES, the main effects of detector acceptance and resolutions as well as the effect of pile-up background were included in the analysis procedure. Based on the established selection procedure of the semileptonic

decay of the $t\bar{t}$ pair system, and making use of the exclusive topology of the final state, the procedure described in Ref. [9] has been developed further by searching for an optimal area in the space of central mass system measured by FPDs and by central detector and in the space of proton transverse momenta measured on both sides of FPDs. With this improved selection procedure we investigated potential in separating the individual (semi)exclusive processes while considering all remaining ones as backgrounds. The inclusive $t\bar{t}$ production overlaid with pile-up remains the most dangerous background for $\langle\mu\rangle$ of 50 and 200. Although compared to results of Ref. [9] significances for individual processes improved, still they do not exceed values of 0.1 in the case of the $\gamma\gamma$ process whose cross section is predicted to be extremely low, and values of 2.0 in the case of the $\mathbb{P}\mathbb{P}$ process whose cross section is about a half of that for the $\gamma\mathbb{P}$ process but whose characteristics in key observables are strikingly similar to those for $\gamma\mathbb{P}$. The best significance of 3.4 was obtained for the $\gamma\mathbb{P}$ process for the lowest pile-up scenario giving thus promising prospects to study this process, which is theoretically well under control, for the first time at LHC and in much detail. Outlooks are also favorable for extraction of the sum of the $\gamma\mathbb{P}$ and $\mathbb{P}\mathbb{P}$ processes. While significance reaches almost 5.0 for low pile-up contaminations, its observation seems to be possible at HL-LHC conditions.

Our results indicate that the discovery of the elastic top pair production in pp collisions at the LHC is feasible and that it is possible to probe, for the first time, the diffractive photoproduction of top quark pairs. Such a perspective strongly motivates the search for new physics beyond the Standard Model in this process, which we plan to discuss in a forthcoming publication. We are convinced that studying the semiexclusive production of such a complex system as the $t\bar{t}$ pair can be considered a solid part of the physics program of forward proton detectors at LHC and HL-LHC.

ACKNOWLEDGMENTS

The authors acknowledge a useful discussion with Michelangelo Mangano during the LHC Top WG meeting and thank Michelle Selvaggi for the help with the DELPHES card used by the CMS Collaboration at HL-LHC. This work was partially financed by the Brazilian funding agencies CNPq (Process No. 164609/2020-2), FAPERGS and INCT-FNA (Process No. 464898/2014-5). M. T. is supported by MEYS of the Czech Republic within Project No. LTT17018.

[1] U. Husemann, Prog. Part. Nucl. Phys. **95**, 48 (2017).
[2] S. Fayazbakhsh, S. T. Monfared, and M. Mohammadi Najafabadi, Phys. Rev. D **92**, 014006 (2015).
[3] G. Aad *et al.* (ATLAS Collaboration), J. High Energy Phys. 11 (2019) 150.
[4] G. Aad *et al.* (ATLAS Collaboration), Eur. Phys. J. C **79**, 1028 (2019).
[5] G. Aad *et al.* (ATLAS Collaboration), Eur. Phys. J. C **80**, 528 (2020).
[6] A. M. Sirunyan *et al.* (CMS Collaboration), Phys. Rev. D **97**, 112003 (2018).
[7] A. M. Sirunyan *et al.* (CMS Collaboration), J. High Energy Phys. 04 (2018) 060.
[8] A. M. Sirunyan *et al.* (CMS Collaboration), Eur. Phys. J. C **79**, 368 (2019).
[9] V. P. Gonçalves, D. E. Martins, M. S. Rangel, and M. Tasevsky, Phys. Rev. D **102**, 074014 (2020).
[10] J. Howarth, arXiv:2008.04249.
[11] L. Adamczyk *et al.*, Report Nos. CERN-LHCC-2015-009, ATLAS-TDR-024.
[12] M. Tasevsky (ATLAS Collaboration), AIP Conf. Proc. **1654**, 090001 (2015).
[13] M. Albrow *et al.* (CMS and TOTEM Collaborations), Report Nos. CERN-LHCC-2014-021, TOTEM-TDR-003, CMS-TDR-13.
[14] V. M. Budnev, I. F. Ginzburg, G. V. Meledin, and V. G. Serbo, Phys. Rep. **15**, 181 (1975).
[15] G. Ingelman and P. E. Schlein, Phys. Lett. **152B**, 256 (1985).
[16] J. D. Bjorken, Phys. Rev. D **47**, 101 (1993).
[17] A. Hebecker, Phys. Rep. **331**, 1 (2000); L. Schoeffel, Prog. Part. Nucl. Phys. **65**, 9 (2010); M. G. Albrow, T. D. Coughlin, and J. R. Forshaw, Prog. Part. Nucl. Phys. **65**, 149 (2010).
[18] A. Aktas *et al.* (H1 Collaboration), Eur. Phys. J. C **48**, 715 (2006).
[19] M. G. Ryskin, A. D. Martin, V. A. Khoze, and A. G. Shuvaev, J. Phys. G **36**, 093001 (2009).
[20] J. C. Collins, Phys. Rev. D **57**, 3051 (1998); **61**, 019902(E) (1999).
[21] M. Dyndal and L. Schoeffel, Phys. Lett. B **741**, 66 (2015).
[22] L. A. Harland-Lang, M. Tasevsky, V. A. Khoze, and M. G. Ryskin, Eur. Phys. J. C **80**, 925 (2020).
[23] L. A. Harland-Lang, V. A. Khoze, and M. G. Ryskin, SciPost Phys. **11**, 064 (2021).
[24] M. Luszczak, R. Maciula, and A. Szczurek, Phys. Rev. D **91**, 054024 (2015).
[25] V. P. Goncalves, C. Potterat, and M. S. Rangel, Phys. Rev. D **93**, 034038 (2016).
[26] M. Luszczak, R. Maciula, and A. Szczurek, Phys. Rev. D **84**, 114018 (2011).
[27] V. P. Goncalves, M. M. Jaime, D. E. Martins, and M. S. Rangel, Phys. Rev. D **97**, 074024 (2018).

[28] C. Brenner Mariotto, V. P. Goncalves, and R. Palota da Silva, Phys. Rev. D **98**, 014028 (2018); V. P. Goncalves and R. Palota da Silva, Phys. Rev. D **101**, 034025 (2020).
[29] V. A. Khoze, A. D. Martin, and M. G. Ryskin, Eur. Phys. J. C **18**, 167 (2000).
[30] V. S. Fadin and V. A. Khoze, JETP Lett. **46**, 525 (1987).
[31] A. Czarnecki and K. Melnikov, Phys. Rev. D **65**, 051501 (2002).
[32] Y. Kiyo, J. H. Kuhn, S. Moch, M. Steinhauser, and P. Uwer, Eur. Phys. J. C **60**, 375 (2009).
[33] A. H. Hoang and M. Stahlhofen, J. High Energy Phys. 05 (2014) 121.
[34] J. Piclum and C. Schwinn, J. High Energy Phys. 03 (2018) 164.
[35] H. Abramowicz *et al.* (CLICdp Collaboration), J. High Energy Phys. 11 (2019) 003.
[36] W. L. Ju, G. Wang, X. Wang, X. Xu, Y. Xu, and L. L. Yang, J. High Energy Phys. 06 (2020) 158.
[37] G. Cowan, K. Cranmer, E. Gross, and O. Vitells, Eur. Phys. J. C **71**, 1554 (2011); **73**, 2501(E) (2013).
[38] M. Boonekamp *et al.*, arXiv:1102.2531.
[39] J. Alwall, M. Herquet, F. Maltoni, O. Mattelaer, and T. Stelzer, J. High Energy Phys. 06 (2011) 128.
[40] T. Sjöstrand, S. Ask, J. R. Christiansen, R. Corke, N. Desai, P. Ilten, S. Mrenna, S. Prestel, C. O. Rasmussen, and P. Z. Skands, Comput. Phys. Commun. **191**, 159 (2015).
[41] J. de Favereau, C. Delaere, P. Demin, A. Giammanco, V. Lemaître, A. Mertens, and M. Selvaggi (DELPHES 3 Collaboration), J. High Energy Phys. 02 (2014) 057.
[42] DELPHES card for CMS at HL-LHC, https://github.com/recotoolsbenchmarks/DelphesNtuplizer/blob/master/cards/CMS_PhaseII_200PU_Snowmass2021_v0.tcl.
[43] L. A. Harland-Lang, V. A. Khoze, M. G. Ryskin, and M. Tasevsky, J. High Energy Phys. 04 (2019) 010.
[44] M. Tasevsky, Int. J. Mod. Phys. A **29**, 1446012 (2014).
[45] K. Cerny, M. Tasevsky, T. Sykora, and R. Zlebcik, J. Instrum. **16**, P01030 (2021).
[46] G. Aad *et al.* (ATLAS Collaboration), Report No. ATL-FWD-PUB-2021-002.
[47] G. Aad *et al.* (ATLAS Collaboration), Phys. Rev. Lett. **125**, 261801 (2020).